

# Description of the FDML Laser with Quasi-steady State Model of the SOA

Zhi Wang, Limei Zhang, Lanlan Liu, Zhenchao Sun, Yingfeng Liu, Fu Wang

Institute of Optical Information, School of Science, Beijing, Jiaotong University,  
Key Laboratory of Luminescence and Optical Information, Ministry of Education, Beijing, China  
Email: zhiwang@bjtu.edu.cn

Received 2013

## ABSTRACT

Experiments and simulations demonstrate that an SOA-based ring cavity can operate as a tunable laser, wavelength-swept laser or Fourier-domain-mode-locking laser according to the relation between the roundtrip frequency and the sweeping frequency of the filter.

**Keywords:** Mode Locked Laser; Semiconductor Optical Amplifiers; Tunable Filter

## 1. Introduction

In the Fourier Domain Mode Locking laser (FDML), which was first presented by R. Huber [1,2], a narrowband optical band pass filter is driven in resonance with the optical roundtrip time of the laser cavity. The required resonator length of several kilometers is realized by a long delay line consisting of single mode fiber (SMF) and dispersion management fibers. As each wavelength component circulates in the cavity such that it is transmitted through the filter at every pass, FDML represents a stationary operating regime. Lasing does not have to build up repetitively as in conventionally wavelength swept laser (WSL) sources, resulting in improved noise performance, coherence length, output power and higher maximum sweep repetition rates [1].

In spite of the numerous applications of FDML lasers demonstrated [3-8] so far, up to now, only one model for the theoretical description of FDML is proposed by Christian Jirauschek [9]. In their model, a dynamic equation is derived to identify the physical effects relevant for FDML, and clarify the role of amplified spontaneous emission (ASE) for self-starting and for the steady state operation of FDML lasers. In 2012, they employed a numerical simulation based on this model to investigate the temporal evolution of the instantaneous power spectrum at different points in the laser cavity, and gained deeper insight into the role of the physical effects governing FDML dynamics, such as gain recovery and linewidth enhancement in the SOA, dispersion and self-phase modulation (SPM) in the optical, and the filter sweeping action [10].

However, there are a few defaults in Christian's model, and a novel mechanism for SOA-based ring cavity

FDML laser (SOA-R-FDML) will be established based on the quasi-steady state SOA [11] in this manuscript. The improvement mainly comes from four aspects: first, frequency dependence of the spectral gain (including the material gain and absorption) are considered; second, the gain properties of the SOA is simulated based on the steady state model, which can give us the gain characteristics for any incident frequency and power, including the gain saturation; third, the ASE is always included in the steady state model, accompanying with the resonance light in the cavity and in the SOA; fourth, the FP transmission function is used to accurately describe the sweep filter.

## 2. Building up Laser Activity

**Figure 1(a)** is the basic structure of the SOA-R-FDML, in which the SOA is the gain medium, the tunable filter is driven by external signal, the coupler is for feedback and output, isolators (ISO), polarization control (PC), and dispersion management fibers are also included in the cavity.

The cavity length of the SOA-R-FDML is about tens of meters or kilometers, the roundtrip time of light in the cavity is about hundreds of ns or us. The experiments show that tens of roundtrips is necessary to build up the laser from ASE with the amplifications by the SOA, so it will cost about a few us or ms, which is much longer than the gain recovery time of SOAs, which is about hundreds of ps, so the SOA can be modeled as a steady-state element.

When the injection current of the SOA is 200 mA, the cavity is 20 m long, and the coupler is 70:30 (feedback :

output), the FWHM of the filter is about 0.146nm @ 1560.52 nm, the building up activity in the SOA-R-FDML can be simulated and shown in **Figure 2**. **Figure 2(a)** shows the output spectra when the roundtrip is 1, 5, 10, 15, 20 and 50. **Figure 2(b)** shows the dependence of the output peak power and the FWHM on the roundtrip in the cavity, and the inset is the measured stationary spectra. **Figure 2(c)** shows the relationship between the output peak power (normalized to the saturation power of the SOA) and the roundtrip, and the inset is the results (by OSC) where every step corresponds to every roundtrip. From these figures, it can be seen that the peak power increases and the linewidth becomes narrower till to be unchanged after enough roundtrips, the cavity will be a stationary laser with the output power of about 9.14 dBm and the FWHM of about 0.054 nm. It can be counted from **Figure 2(c)** that the roundtrip is only 16 or 8 if the laser output about 95% or 80%, and the experiments show that about 12 roundtrips (i.e. 12 steps) is sufficient for lasing.

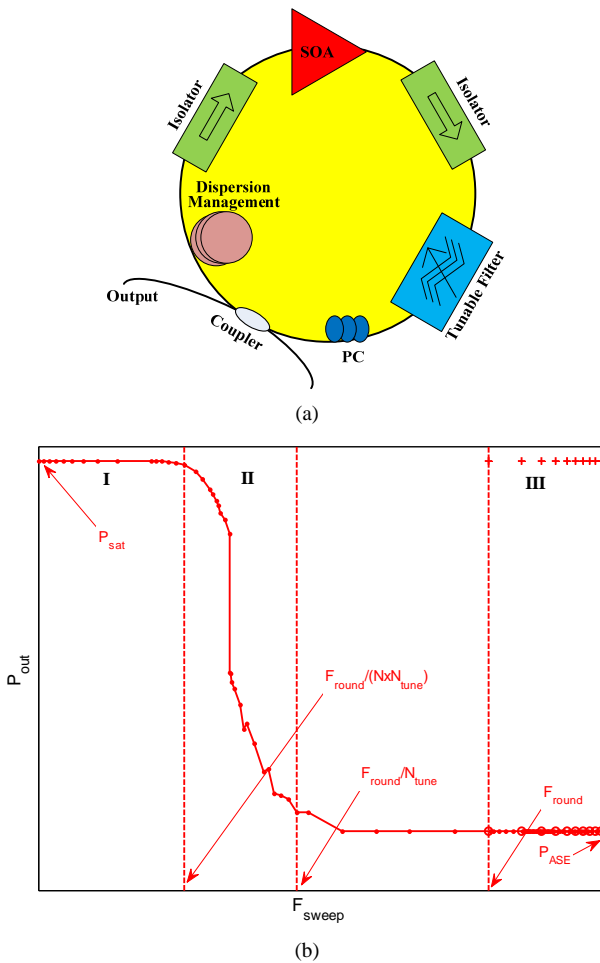
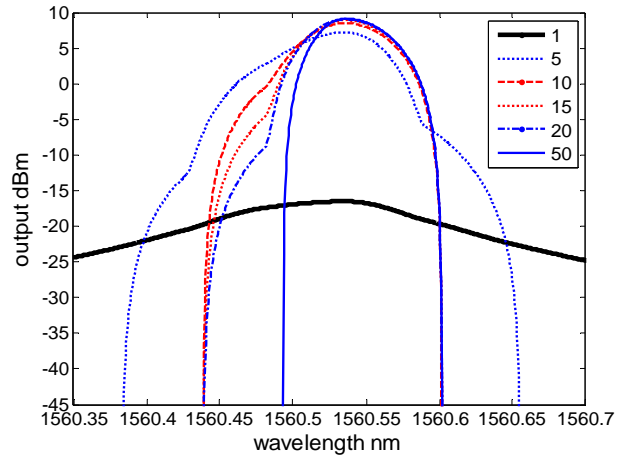
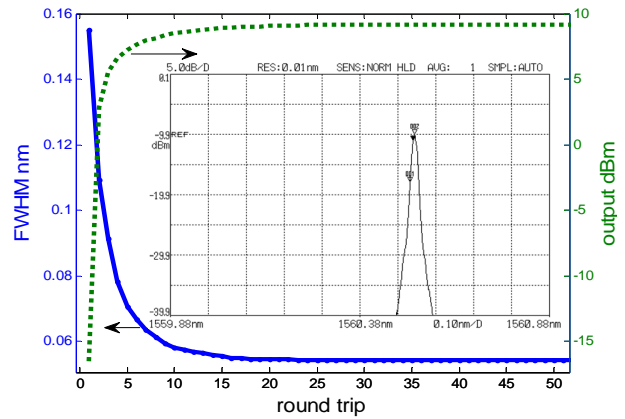


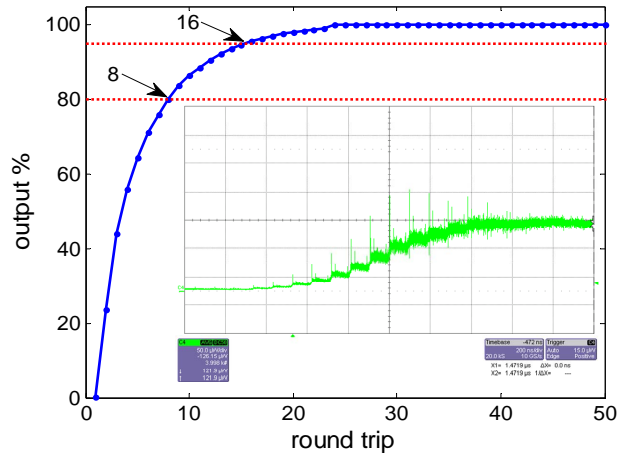
**Figure 1.** (a) Structure of the SOA-R-FDML, (b) relationship between the output peak power of the ring cavity and the full band sweeping frequency.



(a)



(b)



(c)

**Figure 2.** Building up laser activity in the cavity, (a) is the evolution of the spectra, (b) is the evolution of the peak power and the FWHM, (c) is the evolution of the normalized peak power.

### 3. Three Operation Regimes

The center wavelength of the tunable filter varies with

time, and can be written as Eq. (1) for linear or sinusoidal driver, where  $\Delta\lambda_{sweep}=\lambda_{max}-\lambda_{min}$ ,  $\lambda_{avg}=(\lambda_{max}+\lambda_{min})/2$ ,  $\lambda_{min}$  and  $\lambda_{max}$  are the min and max wavelength within the tuning band,  $\text{mod}(t, T_{sweep})$  is the modulus after  $t$  divided by  $T_{sweep}$ ,  $F_{sweep}$  ( $=1/T_{sweep}$ ) is the full band sweeping frequency.

$$\lambda(t)_{linear} = \lambda_{min} + F_{sweep} \cdot \text{mod}(t, T_{sweep}) \cdot \Delta\lambda_{sweep}$$

$$\lambda(t)_{sin} = \lambda_{avg} + \sin\left[2\pi F_{sweep} \cdot \text{mod}(t, T_{sweep}) - \pi/2\right] \cdot \Delta\lambda_{sweep} / 2$$

For the ring cavity, the laser can be built up from the ASE of the SOA after  $N$ -times amplifications (the gain is usually not same), it is also to say that light must propagate  $N$  roundtrips in the cavity for lasing, so the building up time can be written as  $T_{build} = NT_{round}$  (building up frequency  $F_{build} = F_{round}/N$ ), where  $T_{round}$  is the roundtrip time of the light (roundtrip frequency  $F_{round} = 1/T_{round}$ ). The effective tuning times in from  $\lambda_{min}$  to  $\lambda_{max}$  is  $N_{tune} = \Delta\lambda_{sweep}/\Delta\lambda_{FWHM}$ , where  $\Delta\lambda_{FWHM}$ , the FWHM of the tunable filter, is considered as the sweeping wavelength resolution for the ring cavity, and the sweeping time resolution is  $T_{FWHM} = T_{sweep}/N_{tune}$ . The relationship between the output peak power and the full band sweeping frequency  $F_{sweep}$  is obtained by this model and demonstrated in **Figure 1(b)**.

### 3.1. WSL

If  $F_{sweep} \ll F_{round}/(N \cdot N_{tune})$ , the output of the ring cavity is just the saturation power of the gain medium, i.e., it is a tunable laser when the filter is very slowly tuned. If the filter is continuously tuned faster, and  $F_{sweep} < F_{round}/(N \cdot N_{tune})$ , it is a common wavelength swept laser (WSL), the output can be up to the saturation power of the SOA. The region I in **Figure 1(b)** is for the regime of the tunable laser or WSL.

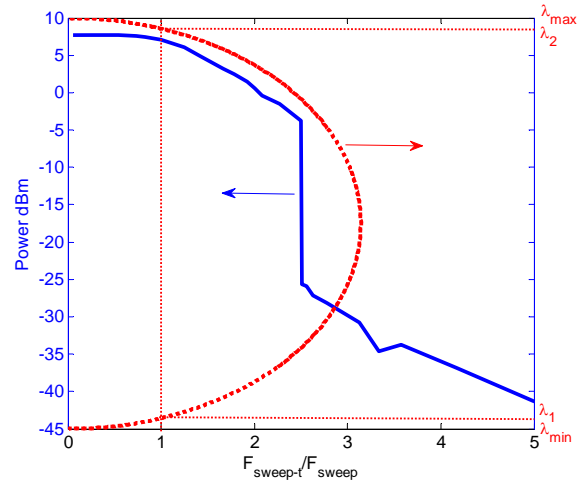
When  $F_{round}/(N \cdot N_{tune}) < F_{sweep} < F_{round}/N_{tune}$ , i.e., the light propagates in the ring cavity less than  $N$  roundtrips, the ASE can't be amplified enough to build up laser, the output peak power will be less than the saturation power with a broad spectra linewidth. The ring cavity does not operate as a laser in this regime, which is shown as the region II in **Figure 1(b)**, and the output power decreases as  $F_{sweep}$  increasing.

If the filter is driven by a sinusoidal wave, the instantaneous sweeping frequency  $F_{sweep\_t}$  at different wavelength can be derived from Eq. (1) and written as Eq. (2).

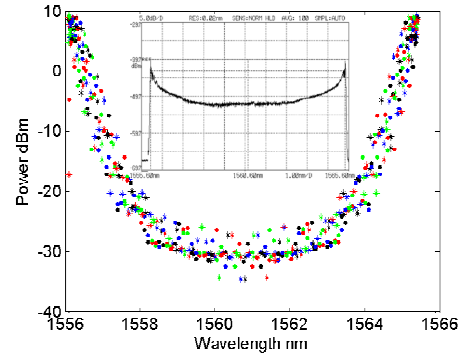
$$F_{sweep\_t}(\lambda) = \pi F_{sweep} \sqrt{1 - 4(\lambda - \lambda_{avg})^2 / \Delta\lambda_{sweep}^2}. \quad (2)$$

$F_{sweep\_t}$  is not exactly equal to  $F_{sweep}$  due to the nonlinearity of the sinusoidal function. The relationship between  $F_{sweep\_t}$  and the wavelength is shown on the right axis of **Figure 3(a)**, and the left axis is a part of **Figure 1(b)**.  $F_{sweep\_t}$  exactly equals to the driven frequency  $F_{sweep}$

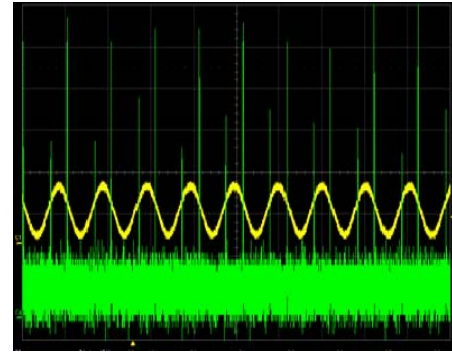
only at wavelength  $\lambda_1$  and  $\lambda_2$ , and higher than  $F_{sweep}$  for the wavelength in the range of  $(\lambda_1, \lambda_2)$  with the maximum  $\pi F_{sweep}$ , for  $\lambda < \lambda_1$  or  $\lambda > \lambda_2$ ,  $F_{sweep\_t}$  is lower than  $F_{sweep}$ . The output power is greater on both end of the sweeping range and smaller in the mid-band, which is shown in **Figure 3(b)**, and the spectra of both simulations and experiments (inset figure) have good agreements.



(a)



(b)



(c)

**Figure 3.** Properties of the WSL while the filter is driven by a sinusoidal, (a) is the relationship between  $F_{sweep\_t}$  and  $\lambda$ , (b) is the spectra of both simulation and experiment, (c) is the drive waveform and output @ 1559.6 nm.

In our setup, the ring cavity is about 12km long, the tunable filter is driven by a sinusoidal function with frequency of 22.34 kHz and  $V_{pp}$  of 2.23 V, the output spectra covers the band from 1556.1nm to 1565.4 nm. **Figure 3(c)** is the waveform recorded by an oscilloscope following a band pass filter @1559.6 nm at the output of the WSL, where the sinusoidal is the driver for the filter, the peak and valley are corresponding to 1556.1 nm and 1565.4 nm, respectively. It shows that forward sweeps (shorter to longer wavelength) have higher energy than backward sweeps, this asymmetry is due to nonlinearities in the SOA which tend to produce a downshift in energy [2].

### 3.2. FDML

When  $F_{sweep} > F_{round}/N_{tune}$ , the ASE is always suppressed by the filter after passing the SOA, so the output power is even less than the ASE, the ring cavity does not work in this regime. But, when  $F_{sweep} = M \times F_{round}$  ( $M = 1, 2, 3, \dots$ ), i.e., the sweeping frequency of the tunable filter is exactly equal to the roundtrip frequency or its  $M^{\text{th}}$  order harmonic, each wavelength component circulates in the cavity such that it is transmitted through the filter and feedback into the SOA for amplifying at every pass, Lasing could build up not as in the conventional WSL. Now, it is so-called Fourier domain mode locking laser (FDML), which is shown as the red '+' in region III in **Figure 1(b)**.

In the simulations, the tunable filter is driven by a sawtooth wave with frequency  $F_{sweep} = F_{round}$ , the wavelength is swept from 1500 nm to 1600 nm, the injection current of the SOA is 260 mA. **Figure 4(a)** shows the relationships between the output peak power and the roundtrip at wavelength 1555 nm, 1560 nm and 1565 nm, it shows that the ring cavity will be a stationary operation FDML after only 5 roundtrips. **Figure 4(b)** shows the evolution of the spectra within a bandwidth of about 10nm, the roundtrip increases from lower to upper, and the inset shows the spectra around 10 dBm. The output of the FDML shows tiny difference between different wavelengths due to the unflatness of the saturation of the SOA, in the simulations, the unflatness is only about 0.03 dB (about 0.7%) near 10dBm.

### 4. Conclusions

Against the current model, a modified model based on the quasi-steady state SOA and segmentation method with discrete frequencies is established for the frequency domain mode locking lasers. With the consideration of the tuning process of the filter and the feedback in the ring cavity, the dynamics of the building up laser activity in the ring cavity are investigated. The relationship between the output peak power  $P_{out}$  and the full band sweeping frequency  $F_{sweep}$  of the tunable filter is obtained

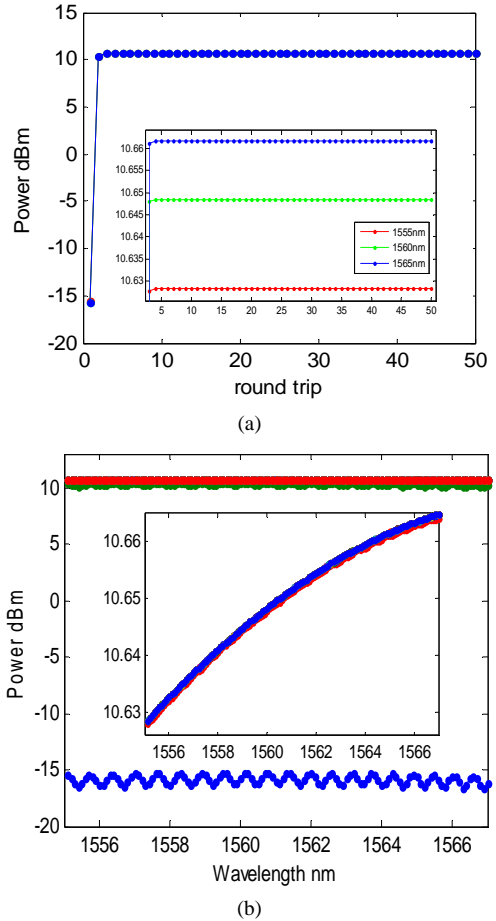


**Figure 4. evolution of the output power (a) and the spectra of the FDML (b).**

with the simulations of the amplified spontaneous emission (ASE) and the gain properties of the SOA. The SOA-R-FDML could operate at three different regimes, which are tunable lasers, wavelength swept lasers (WSL) and FDML lasers according to the relation between the sweeping frequency  $F_{sweep}$  and the round trip frequency  $F_{round}$  in the ring cavity. Some results for WSL and FDML from both simulations and experiments agree well to each other.

### 5. Acknowledgements

This work was supported by the National Natural Science Foundation of China (61077048), Beijing Natural Science Foundation (4132035), Specialized Research Fund for the Doctoral Program of Higher Education (20120009110032), and by Beijing Jiaotong University (2009JBM103, 2012JBM103).

### REFERENCES

- [1] R. Huber, M. Wojtkowski and J. G. Fujimoto, "Fourier Domain Mode Locking (FDML): A New Laser Operating

- Regime and Applications for Optical Coherence Tomography,” *Optics Express*, Vol. 14, 2006, pp. 3225-3237. [doi:10.1364/OE.14.003225](https://doi.org/10.1364/OE.14.003225)
- [2] R. Huber, M. Wojtkowski, K. Taira, J. G. Fujimoto and K. Hsu, “Amplified, Frequency Swept Lasers for Frequency Domain Reflectometry and OCT Imaging: Design and Scaling Principles,” *Optics Express*, Vol. 13, 2005, pp. 3513-3528. [doi:10.1364/OPEX.13.003513](https://doi.org/10.1364/OPEX.13.003513)
- [3] S. W. Huang, A. D. Aguirre, R. A. Huber, D. C. Adler, and J. G. Fujimoto, “Swept Source Optical Coherence Microscopy Using A Fourier Domain Mode Locking Laser,” *Optics Express*, Vol. 15, 2007, pp. 6210-6217. [doi:10.1364/OE.15.006210](https://doi.org/10.1364/OE.15.006210)
- [4] R. Huber, M. Wojtkowski, J. G. Fujimoto, J. Y. Jiang, and A. E. Cable, “Three-Dimensional and C-Mode OCT Imaging with a Compact, Frequency Swept Laser Source at 1300 nm,” *Optics Express*, Vol. 13, 2005, pp. 10523-10538. [doi:10.1364/OPEX.13.010523](https://doi.org/10.1364/OPEX.13.010523)
- [5] R. Huber, D. C. Adler and J. G. Fujimoto, “Buffered Fourier Domain Mode Locking: Unidirectional Swept Laser Sources for Optical Coherence Tomography Imaging at 370,000 lines/s,” *Optics Letters*, Vol. 31, 2006, pp. 2975-2977. [doi:10.1364/OL.31.002975](https://doi.org/10.1364/OL.31.002975)
- [6] M. Wojtkowski, V. Srinivasan, T. Ko, J. Fujimoto, A. Kowalczyk and J. Duker, “Ultrahigh-Resolution, High-Speed, Fourier Domain Optical Coherence Tomography and Methods for Dispersion Compensation,” *Optics Express*, Vol. 12, 2004, pp. 2404-2422. [doi:10.1364/OPEX.12.002404](https://doi.org/10.1364/OPEX.12.002404)
- [7] W. Wieser, B. R. Biedermann, T. Klein, C. M. Eigenwillig and R. Huber, “Multi-megahertz OCT: High Quality 3D Imaging at 20 Million A-Scans and 4.5 GVoxels Per Second,” *Optics Express*, Vol. 18, 2010, pp. 14685-14704. [doi:10.1364/OE.18.014685](https://doi.org/10.1364/OE.18.014685)
- [8] T. Klein, W. Wieser, C. M. Eigenwillig, B. R. Biedermann and R. Huber, “Megahertz OCT for Ultrawide-Field Retinal Imaging with A 1050 nm Fourier Domain Mode-Locked Laser,” *Optics Express*, Vol. 19, 2011, pp. 3044-3062. [doi:10.1364/OE.19.003044](https://doi.org/10.1364/OE.19.003044)
- [9] C. Jirauschek, B. Biedermann and R. Huber, “A Theoretical Description of Fourier Domain Mode Locked Lasers,” *Optics Express*, Vol. 17, 2009, pp. 24013-24019. [doi:10.1364/OE.17.024013](https://doi.org/10.1364/OE.17.024013)
- [10] S. Todor, B. Biedermann, R. Huber and C. Jirauschek, “Balance of Physical Effects Causing Stationary Operation of Fourier Domain Mode-Locked Lasers,” *Journal. Of Optical Society of America B*, Vol. 29, 2012, pp. 656-664. [doi:10.1364/JOSAB.29.000656](https://doi.org/10.1364/JOSAB.29.000656)
- [11] M. J. Connelly, “Wideband Semiconductor Optical Amplifier Steady-State Numerical Model,” *IEEE Journal of Quantum Electronics*, Vol. 37, 2001, pp. 439-447. [doi:10.1109/3.910455](https://doi.org/10.1109/3.910455)